

# Phase behavior of organic-inorganic crystal

## Temperature-dependent diffuse reflectance infrared spectroscopy of silver stearate

S.J. Lee, S.W. Han, H.J. Choi, and K. Kim<sup>a</sup>

School of Chemistry and Molecular Engineering and Center for Molecular Catalysis, Seoul National University, Seoul 151-742, Korea

Received 29 November 2000

**Abstract.** We have investigated the structure and phase behavior of nonmolecularly layered silver stearate by means of temperature-dependent diffuse reflectance infrared Fourier transform (DRIFT) spectroscopy. Upon heating the sample, remarkable spectral changes took place. The first phase transition took place that might be associated with a premelting event characterized by the formation of gauche conformers at 390–420 K. A second phase transition took place in which silver nanoparticles with a size of  $\sim 4$  nm were formed by thermal decomposition of silver stearate at 520–550 K. These silver nanoparticles, derivatized by stearate, were readily spread as a monolayer at air/water interface, and could be packed in 3-D assemblies by the Langmuir-Blodgett method.

**PACS.** 81.07.Pr Organic-inorganic hybrid nanostructures – 61.46.+w Nanoscale materials: clusters, nanoparticles, nanotubes, and nanocrystals

## 1 Introduction

It has been found recently that silver alkane thiolate salt (AgSR) consists of an infinite-sheet, two-dimensional (2-D), nonmolecular layered structure [1–4]. The alkyl chains even in  $\text{AgS}(\text{CH}_2)_4\text{CH}_3$  possess fully-extended all-trans conformation [1]. Silver alkane carboxylate salt ( $\text{AgCO}_2\text{R}$ ) was also reported to consist in a layered structure [5]. Its detailed structural characteristics have not yet been thoroughly elucidated, however. Owing to their similar structures, the properties of  $\text{AgCO}_2\text{R}$  are expected to be similar to those of AgSR. The layered AgSR species are known to show liquid crystalline behavior upon melting [2]. This phenomenon is associated with the two structural motifs that the coordination of Ag to thiolates changes from trigonal to diagonal and that the interlayer  $\text{CH}_3$ - $\text{CH}_3$  contacts disrupt to form stacked-disk micellar structures. These organic-inorganic heterostructures have attracted interest since technologically relevant materials with specific properties should be readily prepared by systematic variation in the structure and properties of the organic and inorganic constituents at the molecular level [6–8]. In particular,  $\text{AgCO}_2\text{R}$  is known to be decomposed into silver nanoparticles [9]. In this respect, we have investigated the structure and phase behavior of the prototype  $\text{AgCO}_2\text{R}$ , silver stearate ( $\text{AgCO}_2(\text{CH}_2)_{16}\text{CH}_3$ ), by means of temperature-dependent diffuse reflectance infrared Fourier transform (DRIFT) spectroscopy. It has

been attempted to differentiate similarity as well as dissimilarity of the structural properties between  $\text{AgCO}_2\text{R}$  and AgSR.

## 2 Experimental

### 2.1 Preparation of silver stearate

Stearic acid (99+%) and silver nitrate (99+%) were purchased from Aldrich and used as received. Unless specified, other chemicals were reagent grade, and triply-distilled water (resistivity greater than 18 M cm) was used throughout. Silver stearate was prepared by two-phase method. An aqueous solution of  $\text{AgNO}_3$  was added dropwise to stearic acid solution dissolved in toluene. After 3 hrs of vigorous stirring, the resulting bright-yellowish solid was filtered, washed subsequently with ethanol, toluene and cold water in order, and finally dried under vacuum.

### 2.2 Characterization

X-ray diffraction (XRD) patterns were obtained with a Rigaku Dmax-3C diffractometer for a  $2\theta$  range of  $5^\circ$  to  $50^\circ$  at an angular resolution of  $0.05^\circ$  using  $\text{Cu K}\alpha$  ( $1.5418 \text{ \AA}$ ) radiation. Infrared spectra were measured using a Bruker IFS 113v FT-IR spectrometer. The method for obtaining the room temperature and temperature-dependent

<sup>a</sup> e-mail: kwankim@plaza.snu.ac.kr

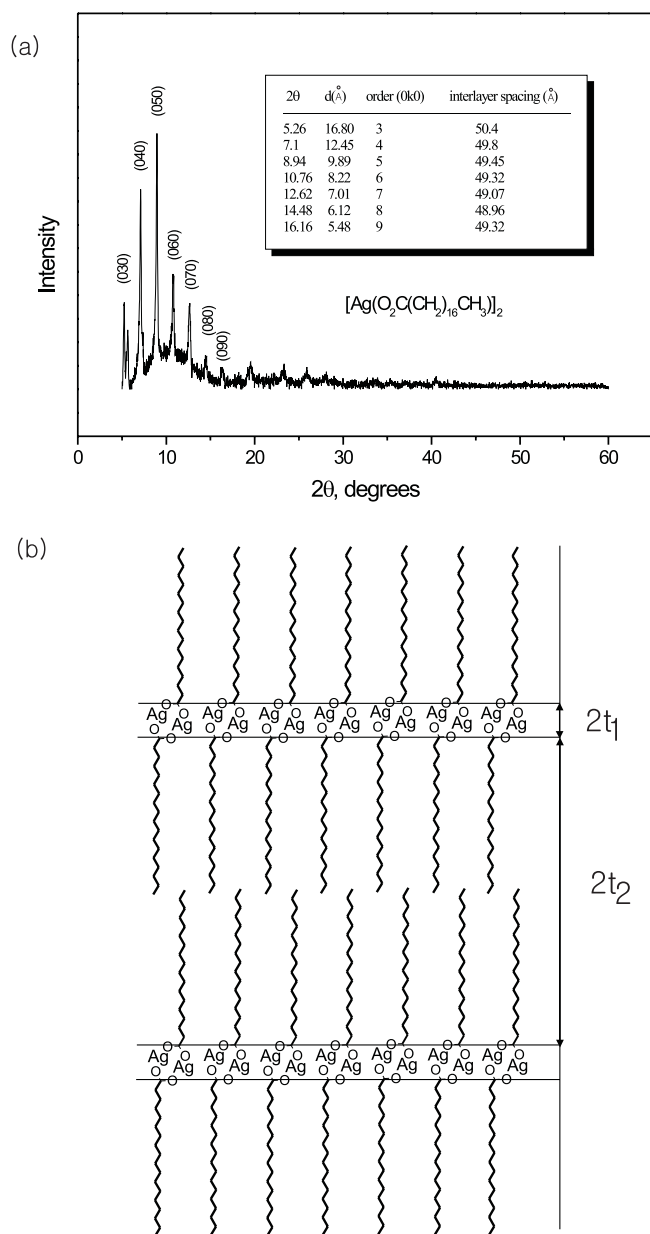


**Fig. 1.** (a) XRD pattern of silver stearate. (b) Structure of silver stearate.

DRIFT spectra has been reported previously [10]. Transmission electron micrograph of the thermally decomposed sample was obtained with a JEM-200CX transmission electron microscope (TEM) at 160 kV after placing a drop of toluene solution on carbon-coated copper grids (150 mesh). The UV/Vis spectrum of thermally decomposed sample was taken in toluene solvent with a SCINCO S-2130 spectrophotometer. Monolayers of the thermally decomposed sample at air/water interface were characterized by a KSV 3000 Langmuir balance.

## 3 Result and discussion

### 3.1 Structure of silver stearate

Fig. 1(a) shows the XRD data for silver stearate. Known from 1950 [5], the compound shows a well-developed progression of intense reflections. These intense reflections can be interpreted in terms of three dimensionally stacked silver carboxylate layers with a large interlayer lattice dimension. Each layer of silver carboxylate is separated from the other by twice the length of the alkyl chain. In this sense, all intense reflections can be indexed as (0k0) and the reflections are assigned in Fig. 1(a). In the inset of Fig. 1(a), we list the interlayer spacings derived from different reflections. The averaged interlayer spacing is 49.47 Å. Following the Ag K-EXAFS studies of Tolochko *et al.* [11], the thickness of the Ag-O slab, *i.e.*,  $2t_1$  in Fig. 1(b), could be estimated to be 4.91 Å. Considering that the averaged interlayer spacing derived from Fig. 1(a) was 49.47 Å, the thickness of the alkyl chain layer, *i.e.*,  $2t_2$  in Fig. 1(b), should then be 44.56 Å. Assuming that the alkyl chains in silver stearate are fully extended and all-trans (*vide infra*) and invoking the known bond lengths and vdW radii, the chain length from the carboxylate carbon atom to the terminal methyl group should be 22.99 Å. Twice of the latter is 45.98 Å, which is 1.42 Å longer than that derived from the measured XRD data, *i.e.*, 44.56 Å. The estimated difference indicates that the extent of overlap between the adjacent layers, if exists, is small. A similar conclusion is made for silver alkanethiolate; the extent of interpenetration has been reported to be 0.5 Å [4]. The overall structure of silver stearate as drawn in Fig. 1(b) is supposed to be quite similar to that of silver alkanethiolate.

### 3.2 DRIFT spectral features of silver stearate

Fig. 2 shows a series of DRIFT spectra obtained as a function of temperature for silver stearate. The high frequency region of 2750-3050  $\text{cm}^{-1}$  reveals the C-H stretching modes of the methyl and the methylene groups of stearate while the low frequency region of 1000-1800  $\text{cm}^{-1}$  displays the stretching modes of the carboxylate group as well as the scissoring, rocking, wagging, and twisting modes of the methylene groups. It can be evidenced from the room temperature spectrum that the obtained sample is not contaminated with free acid and the alkyl chains in silver stearate are in an all-trans conformational state with little or no significant gauche population as in silver alkanethiolate. (The two strong peaks observed at 2848 and 2916  $\text{cm}^{-1}$  in Fig. 2(a) are assigned to the symmetric ( $\nu_s(\text{CH}_2)$ ,  $d^+$ ) and the asymmetric ( $\nu_{as}(\text{CH}_2)$ ,  $d^-$ ) stretching vibrations of the methylene groups, respectively. These modes usually lie in the narrow ranges of 2846-2850 and 2915-2918  $\text{cm}^{-1}$ , respectively, for all-trans extended chains [12] (*vide supra*) and in the distinctly different ranges of 2854-2856 and 2924-2928  $\text{cm}^{-1}$  for disordered chains [13].) The fact that only a single narrow band

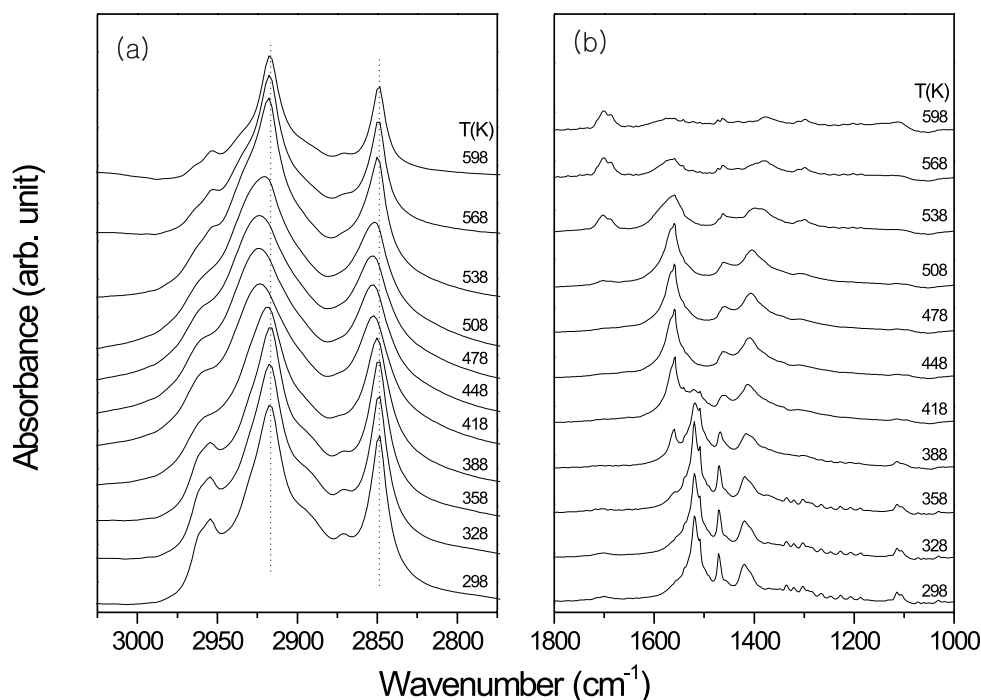


**Fig. 2.** DRIFT spectra of silver stearate taken as a function of temperature: (a) high and (b) low frequency regions.

(fwhm  $\sim 5.9 \text{ cm}^{-1}$ ), which can be attributed to the scissoring vibration of the methylene group ( $\delta(\text{CH}_2)$ ), is observed at  $1471 \text{ cm}^{-1}$  also suggests that silver stearate consists in triclinic packing with two chains per unit cell [14]. This infrared data is consistent with the reported X-ray analysis on a number of silver carboxylates [5]. Shown in Fig. 2(a), the thermotropic upwards shifts of methylene stretching bands from 390 to 420 K can be attributed to a premelting event characterized by the formation of gauche conformers. The frequency change of  $\delta(\text{CH}_2)$  is abrupt around 420 K appearing at  $1463 \text{ cm}^{-1}$  as shown in Fig. 2(b). The thermal variation of  $\delta(\text{CH}_2)$  band observed herein suggests that a triclinic chain packing disrupts around 420 K to hold a hexagonal packing [14]. Interestingly, the frequencies of  $d^+$  and  $d^-$  modes sharply decrease from 2853 and  $2923 \text{ cm}^{-1}$  at 520 K to 2848 and  $2916 \text{ cm}^{-1}$  at 550 K; the latter values are nearly the same as those at room temperature. As to be discussed later, this results from the formation of stearic acid-derivatized silver nanoparticles. Above 550 K, the relative intensities of all infrared bands gradually decrease, and the intensities at 600 K are observed to be below half of the initial values at 298 K. Such lowering of the intensities is attributed to the thermal decomposition of silver stearate to produce various products including metallic silver,  $\text{CO}_2$ , stearic acid, and paraffins [15].

### 3.3 Thermal decomposition of silver stearate

The composition of the products of the thermal decomposition of silver carboxylates depends on reaction conditions, including such factors as the surrounding atmo-

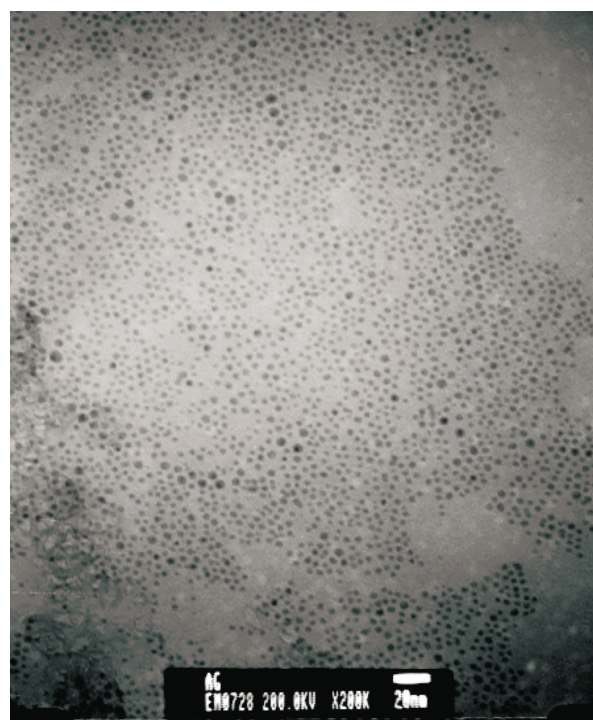


**Fig. 3.** TEM image of stearate-derivatized Ag nanoparticles.

sphere, heating rate, and temperature. Andreev *et al.* [15] reported that thermal decomposition of silver stearate led to metallic silver,  $\text{CO}_2$ , stearic acid, and paraffins. On the other hand, Uvarov *et al.* [16] reported that silver stearate showed phase transitions at 397 K and 426 K in air. The

former transition was claimed to be irreversible leading to decreased conductivity while the latter was accompanied by the thermal decomposition leading to increased conductivity. Free stearic acid was presumed to be one of the decomposition products. In the present work, the first phase transition is observed to occur in the range from 390 K to 420 K. Above 510 K, the C=O stretching peak is clearly identified at  $\sim 1700\text{ cm}^{-1}$ ; the peak must arise from a free acid as suggested by Uvarov *et al.* Recently, Abe *et al.* [9] reported that thermal decomposition of silver stearate at 523 K in an atmosphere of  $\text{N}_2$  should produce silver nanoparticles with a size of 5 nm. In fact, the latter temperature corresponds to that of the second phase transition in the present work, *i.e.*, 520–550 K. On these grounds, we have conducted TEM measurement for a sample of silver stearate heated to 520 K for 10 min and then rinsed in methanol; the rinsed sample was readily dispersed in non-polar medium such as toluene. Fig. 3 shows the TEM image of the sample taken after vaporizing the toluene solvent on the surface of copper grid. The image reveals that silver nanoparticles are indeed formed by the thermal decomposition of silver stearate. The sizes of the nanoparticles are quite uniform with an average diameter of  $\sim 4$  nm. The distance between nanoparticles is estimated to be 3–3.5 nm. Recalling that the chain length of stearic acid is  $\sim 1.7$  nm, silver nanoparticles are thus supposed to be surrounded by stearate. A distinct peak was observed at 417 nm in the UV/Vis spectrum, which must arise from the surface plasmon absorption of silver nanoparticles [17]. We can confirm from DRIFT spectroscopy that the silver nanoparticles are indeed passivated by uniform surroundings of stearate of which alkyl chains assume fully-extended all-trans conformation. From the TEM image, it is evident that stearate-derivatized silver nanoparticles are readily condensed to form two-dimensional arrays. On these grounds, we firstly spread silver nanoparticles on the water subphase of a LB film balance and recorded the surface pressure as a function of surface area. The isotherm appears to consist of liquid expanded, liquid condensed, and their composite plateau regions. It is remarkable that the collapse pressure reaches up to 59 mN/m; the collapse pressure for stearic acid on pure water (at pH  $\sim 6$ ) at 293 K is only  $\sim 50$  mN/m and it increases to  $\sim 59$  mN/m at pH 9.0 [18]. This may indicate that energetically favorable interdigitated structure is formed to maximize the hydrophobic interaction between the interdigitated chains. A more detailed study on the structure and the intermolecular interaction of the nanoparticles at an air/water interface and in 3-D assemblies is under progress.

#### 4 Summary and conclusion

The structure and phase behavior of silver stearate have been investigated by DRIFT spectroscopy. We confirmed by XRD analysis that silver stearate consisted of an infinite sheet, 2-D, nonmolecular layered structure. The alkyl chains in silver stearate were in an all-trans conformational state with little or no significant gauche popula-

tion as in silver alkanethiolate. Upon heating the sample, remarkable spectral changes took place. The first phase transition took place that might be associated with a premelting event characterized by the formation of gauche conformers. A second phase transition took place in which silver nanoparticles with a size of  $\sim 4$  nm were formed by thermal decomposition of silver stearate. These nanoparticles were readily spread as a monolayer at air/water interface. Considering that organic-inorganic hetero-structures have recently been attracting immense interest, the present observations should prove useful in developing technologically relevant materials with specific properties by systematic variation of the structure and properties of organic and inorganic constituents at the molecular level.

KK was supported by the Korea Research Foundation (KRF, 042-D00073) and by the Korea Science and Engineering Foundation (KOSEF, 1999-2-121-001-5). SWH was supported by KOSEF through the Center for Molecular Catalysis at Seoul National University. SJL and HJC acknowledge the KRF for providing the BK21 fellowship.

#### References

1. I.G. Dance, K.J. Fisher, R.M.H. Banda, M.L. Scudder, *Inorg. Chem.* **30**, 183 (1991).
2. M.J. Baena, P. Espinet, M.C. Lequerica, A.M. Levelut, *J. Am. Chem. Soc.* **114**, 4182 (1992).
3. F. Bensebaa, T.H. Ellis, E. Kruss, R. Voicu, Y. Zhou, *Langmuir* **14**, 6579 (1998).
4. A.N. Parikh, S.D. Gilmor, J.D. Beers, K.M. Beardmore, R.W. Cutts, B.I. Swanson, *J. Phys. Chem. B* **103**, 2850 (1999).
5. F.W. Matthews, G.G. Waren, J.H. Michell, *Anal. Chem.* **22**, 514 (1950).
6. I.A. Aksay, M. Trau, S. Manne, I. Honma, N. Yao, L. Zhou, P. Fenter, P.M. Eisenberger, S.M. Gruner, *Science* **273**, 892 (1996).
7. L.A. Vermeulen, M.E. Thompson, *Nature* **358**, 656 (1992).
8. V. Laget, C. Hornick, P. Rabu, M. Drillon, P. Turek, R.N. Ziessel, *Adv. Mater.* **10**, 1024 (1998).
9. K. Abe, T. Hanada, Y. Yoshida, N. Tanigaki, H. Takiguchi, H. Nagasawa, M. Nakamoto, T. Yamaguchi, K. Yase, *Thin Solid Films* **327**, 524 (1998).
10. S.J. Lee, K. Kim, *Vib. Spectrosc.* **18**, 187 (1998).
11. B.P. Tolochko, S.V. Chernov, S.G. Nikitenko, D.R. Whitcomb, *Nucl. Instrum. Meth. A* **405**, 428 (1998).
12. R.A. MacPhail, H.L. Strauss, R.G. Snyder, C.A. Elliger, *J. Phys. Chem.* **88**, 334 (1984).
13. R.G. Snyder, H.L. Strauss, C.A. Elliger, *J. Phys. Chem.* **86**, 5145 (1982).
14. M. Borja, P.K. Dutta, *J. Phys. Chem.* **96**, 96 (1992).
15. V.M. Andreev, L.P. Burleva, V.V. Boldyrev, Yu.I. Mikhailiv, *Izv. SO AN USSR, SerKhim. Nauk* **2**, 58 (1983).
16. N.F. Uvarov, L.P. Burleva, M.B. Mizen, D.R. Whitcomb, *C. Zou, Solid State Ionics* **107**, 31 (1998).
17. U. Kreibig, M. Vollmer, *Optical Properties of Metal Clusters* (Springer, 1995).
18. A. Ulman, *An Introduction to Ultrathin Organic Films* (Academic Press, 1991).